HHS Public Access

Author manuscript

Sci Immunol. Author manuscript; available in PMC 2018 August 02.

Published in final edited form as:

Sci Immunol. 2018 February 02; 3(20): . doi:10.1126/sciimmunol.aao4013.

Islet-reactive CD8+ T-cell frequencies in the pancreas but not blood distinguish type 1 diabetes from healthy donors

Slobodan Culina[1,2,3,†], **Ana Ines Lalanne**[1,2,3,†], **Georgia Afonso**[1,2,3], **Karen Cerosaletti**[4], **Sheena Pinto**[5], **Guido Sebastiani**[6], **Klaudia Kuranda**[1,2,3], **Laura Nigi**[6], **Anne Eugster**[7], **Thomas Østerbye**[8], **Alicia Maugein**[1,2,3], **James E. McLaren**[9], **Kristin Ladell**[9], **Etienne Larger**[1,2,3,10], **Jean-Paul Beressi**[11], **Anna Lissina**[12,13], **Victor Appay**[12,13], **Howard W. Davidson**[14], **Søren Buus**[8], **David A. Price**[9,15], **Matthias Kuhn**[16], **Ezio Bonifacio**[7], **Manuela Battaglia**[17], **Sophie Caillat-Zucman**[18], **Francesco Dotta**[6], **Raphael Scharfmann**[1,2,3], **Bruno Kyewski**[5], **Roberto Mallone**[1,2,3,10,*], and **the ImMaDiab Study Group**[‡]

[1]INSERM, U1016, Cochin Institute, Paris, France.

[2]CNRS, UMR8104, Cochin Institute, Paris, France.

[3]Paris Descartes University, Sorbonne Paris Cité, Paris, France.

[4]Benaroya Research Institute, Translational Research Program, Seattle, WA 98101, USA.

[5]DKFZ, Division of Developmental Immunology, Heidelberg, Germany.

[6]University of Siena, Department of Medicine, Surgery and Neuroscience, Diabetes Unit and Fondazione Umberto di Mario ONLUS, Toscana Life Sciences, Siena, Italy.

[7]CRTD-DFG Research Center for Regenerative Therapies Dresden, Medical Faculty, Technische Universität Dresden, Dresden, Germany.

[8]Panum Institute, Department of International Health, Immunology and Microbiology, Copenhagen, Denmark.

[9]Division of Infection and Immunity, Cardiff University School of Medicine, Cardiff, UK.

[10]Assistance Publique Hôpitaux de Paris, Service de Diabétologie, Cochin Hospital, Paris, France.

[11]Centre Hospitalier de Versailles André Mignot, Service de Diabétologie, Le Chesnay, France.

[*]Corresponding author: Roberto Mallone, MD PhD – INSERM U1016 Cochin Institute, DeARLab – Cochin-Port Royal Hospital, Cassini Building – 123, boulevard de Port Royal, F-75014 Paris, France. Phone: +33-1-76.53.55.83. roberto.mallone@inserm.fr.

[†]S. Culina and A.I. Lalanne are co-first authors.

[‡]Members of the ImMaDiab Study Group are listed in Supplementary Materials

Author contributions: S.C. A.I.L., G.A., K.C., S.P., G.S., K.K., L.N., A.E., T.Ø., J.E.M. and M.K. performed experiments and analyzed data; A.M., K.L., E.L., J.P.B., A.L., V.A., H.W.D., S.B., D.A.P., E.B., M.B., S.C.Z., F.D. and R.S. provided critical reagents, experimental assistance and intellectual input; M.K. and R.M. performed statistical analyses; S.C., A.I.L., G.A., K.C., S.P., D.A.P., B.K. and R.M. designed and interpreted experiments, and wrote the paper; the ImMaDiab Study Group recruited patients and performed clinical phenotyping.

Competing interests: The authors declare that no conflict of interest exists. Some T-cell receptor sequences described herein are covered by Inserm-Transfert patent WO/2017/046335.

Data and materials availability: available materials will be provided with the appropriate material transfer agreement.

[12]Pierre et Marie Curie Paris 6 University, Sorbonne Paris Cité, DHU FAST, CR7, Centre d'Immunologie et des Maladies Infectieuses (CIMI-Paris), Paris, France.

[13]INSERM, U1135, CIMI-Paris, Paris, France.

[14]Barbara Davis Center for Diabetes and Integrated Department of Immunology, University of Colorado Denver Anschutz Medical Campus, Aurora, CO 80045, USA.

[15]Vaccine Research Center, National Institute of Allergy and Infectious Diseases, National Institutes of Health, Bethesda, MD 20892, USA.

[16]Institut für Medizinische Informatik und Biometrie, Medical Faculty, Technische Universität Dresden, Dresden, Germany.

[17]Diabetes Research Institute, IRCCS San Raffaele Scientific Institute, Milan, Italy.

[18]Assistance Publique Hôpitaux de Paris, Laboratoire d'Immunologie et Histocompatibilité, Hôpital Saint-Louis, Paris, France.

Abstract

The human leukocyte antigen (HLA)-A2-restricted zinc transporter (ZnT)$8_{186–194}$ and other islet epitopes elicit interferon-γ secretion by $CD8^+$ T cells preferentially in type 1 diabetes (T1D) patients compared with controls. Here, we show that clonal $ZnT8_{186–194}$-reactive $CD8^+$ T cells express private T-cell receptors and display equivalent functional properties in T1D and healthy subjects. *Ex-vivo* analyses further revealed that $CD8^+$ T cells reactive to $ZnT8_{186–194}$ and other islet epitopes circulate at similar frequencies and exhibit a predominantly naïve phenotype in age-matched T1D and healthy donors. Higher frequencies of $ZnT8_{186–194}$-reactive $CD8^+$ T cells with a more antigen-experienced phenotype were detected in children *vs.* adults, irrespective of disease status. Moreover, some $ZnT8_{186–194}$-reactive $CD8^+$ T-cell clonotypes were found to cross-recognize a *Bacteroides stercoris* mimotope. While ZnT8 was poorly expressed in thymic medullary epithelial cells, variable thymic expressions levels of islet antigens did not modulate the peripheral frequency of their cognate $CD8^+$ T cells. In contrast, $ZnT8_{186–194}$-reactive cells were enriched in the pancreata of T1D donors *vs.* non-diabetic and type 2 diabetic controls. Thus, islet-reactive $CD8^+$ T cells circulate in most individuals, but home to the pancreas preferentially in T1D patients. We conclude that the activation of this common islet-reactive T-cell repertoire and progression to T1D likely require defective peripheral immunoregulation and/or a pro-inflammatory islet microenvironment.

Introduction

In the setting of type 1 diabetes (T1D), insulitic lesions are enriched for $CD8^+$ T cells, which are held as the final mediators of islet destruction. Concordantly, preproinsulin (PPI)-reactive $CD8^+$ T-cell clones can lyse β cells *in-vitro* (1), and β-cell-reactive $CD8^+$ T cells infiltrate the islets of T1D patients (2). Autoimmune $CD8^+$ T cells may therefore provide new biomarkers for disease staging complementary to auto-antibodies (aAbs). While interferon (IFN)-γ-secreting $CD8^+$ T cells detected by enzyme-linked immunospot (ELISpot) distinguish T1D patients from healthy donors (3), the situation is more complex when non-functional human leukocyte antigen (HLA) Class I multimer (MMr) assays are

used. Although MMr^+CD8^+ T cells were often (4), but not invariably (5, 6), found at similar frequencies in both T1D and healthy subjects, they have been reported to exhibit more differentiated effector/memory phenotypes (4, 6) in T1D patients. A rather enigmatic state of 'benign' autoimmunity therefore exists in healthy individuals.

We therefore aimed to determine the key features of islet-reactive $CD8^+$ T cells that associate with T1D. We focused our efforts on well-defined HLA-A*02:01 (HLA-A2)-restricted immunodominant epitopes derived from PPI, glutamic acid decarboxylase (GAD), insulinoma-associated protein-2 (IA-2), and islet-specific glucose-6-phosphatase catalytic subunit-related protein (IGRP) (3), and on a highly immunoprevalent zinc transporter $(ZnT)8_{186–194}$ epitope that we recently described (7). The results indicate that incomplete central tolerance mechanisms allow the survival of an islet-reactive $CD8^+$ T-cell repertoire, which in some individuals may be primed in the presence of defective peripheral immunoregulation and/or a pro-inflammatory islet microenvironment to progress toward T1D.

Results

$ZnT8_{186–194}$-reactive $CD8^+$ T-cell clones from T1D and healthy donors display equivalent functionality

Given that $ZnT8_{186–194}$-reactive IFN-γ responses are highly prevalent in T1D patients (7), we started by generating $ZnT8_{186–194}$-reactive $CD8^+$ T-cell clones from a new-onset T1D patient (D222D) (7). Following *in-vitro* expansion with the $ZnT8_{186–194}$ peptide (8), HLA-A2 MMr^+ cells were labeled with two different fluorochromes (9) and sorted (Fig. 1A). The 3 clones thus generated stained uniformly positive with $ZnT8_{186–194}$ MMrs (Fig. 1B) and responded to $ZnT8_{186–194}$ peptide stimulation by secreting tumor necrosis factor (TNF)-α (Fig. 1C), IFN-γ, interleukin (IL)-2 and, to a lesser extent, macrophage inflammatory protein (MIP)-1β in a dose-dependent fashion (Fig. S1A–C). Cytotoxicity was then tested against an HLA-$A2^+$ Epstein-Barr virus (EBV)-transformed B-lymphoblastoid cell line (LCL) pulsed with the cognate $ZnT8_{186–194}$ peptide. Increasing numbers of clonal $CD8^+$ T cells led to the complete disappearance of $ZnT8_{186–194}$-pulsed but not control-pulsed targets, with ≥90% lysis at a 1/2 effector/target (E/T) ratio (Fig. 1D–E and S1D–F). This lytic activity was mostly perforin-mediated (Fig. 1F), as it was inhibited significantly by concanamycin A, marginally by brefeldin A (suppressing cytokine secretion) and not at all by a blocking anti-FasL mAb (suppressing Fas-dependent cytotoxicity), and it was associated with CD107a upregulation (Fig. 1G).

Additional $ZnT8_{186–194}$-reactive $CD8^+$ T-cell clones were generated from other T1D patients and healthy donors. The final panel comprised 16 clones (9 clones from 5 T1D patients and 7 clones from 5 healthy donors), most of which were isolated directly *ex-vivo* (Table S1). All but one clone (H328C 9B3) stained with HLA-A2 MMrs loaded with $ZnT8_{186–194}$ (VAANIVLTV), and several of them also with a longer $ZnT8_{185–194}$ variant (AVAANIVLTV) reported to exhibit similar immunoprevalence (Fig. S2A) (10). Higher staining intensities were observed with $ZnT8_{186–194}$ MMrs for all clones barring D010R 1D3. Concordantly, $ZnT8_{186–194}$ bound to recombinant HLA-A2 molecules with higher affinity (K_D 15 nM *vs.* 207 nM) and similar stability ($t_{1/2}$ 1.8 h *vs.* 2.3 h) relative to the

longer ZnT8$_{185–194}$ peptide (Fig. S2B–C). The ZnT8$_{186–194}$ epitope was therefore retained for subsequent experiments, except for clone D010R 1D3.

Clones from T1D and healthy donors were first compared for the intensity of ZnT8$_{186–194}$ MMr staining. The tyrosine kinase inhibitor dasatinib, which stabilizes T-cell receptor (TCR) interactions with peptide-HLA complexes (11), enhanced MMr staining, particularly for MMr^{low} clones (Fig. 2A). Heterogeneous staining patterns were observed when comparing normalized MMr fluorescence intensities (Fig. 2B). While dasatinib reduced variability, even in its absence no difference was apparent between the T1D and healthy group.

Next, we performed *in-vitro* recall assays with increasing ZnT8$_{186–194}$ peptide concentrations. Representative data are shown in Fig. 2C and results summarized in Fig. 2D–E. In line with the MMr staining profiles, the half maximal effective peptide concentration (EC50) required to elicit cytokine responses (TNF-α, IFN-γ, IL-2) and the maximal cytokine responses were again heterogeneous, but not significantly different between T1D and healthy clones (Fig. 2D–E), with one exception noted for the lower MIP-1β EC50 of T1D clones. Clones obtained after *in-vitro* expansion displayed an equivalent range of antigen (Ag) sensitivities, either high (D222D, H017N) or low (H328C), arguing against a bias compared with clones isolated directly *ex-vivo*. Moreover, the polyfunctionality index, which reflects the number of cells secreting multiple cytokines (12), was similar for T1D and healthy clones (Fig. 2F). As expected, EC50 values correlated negatively with MMr staining and polyfunctionality indices (Fig. S3).

Collectively, these results show that ZnT8-reactive CD8$^+$ T cells isolated from T1D and healthy subjects exhibit similar Ag avidity, sensitivity and polyfunctionality.

ZnT8$_{186–194}$-reactive CD8$^+$ T-cell clones from T1D and healthy donors display equivalent β-cell cytotoxicity

To determine if ZnT8$_{186–194}$-reactive CD8$^+$ T cells can recognize naturally processed ZnT8 epitopes, we performed cytotoxicity assays using ZnT8-transduced K562-A2 targets (K562-A2/ZnT8). High avidity ZnT8$_{186–194}$-reactive clones lysed unpulsed K562-A2/ZnT8 targets almost as efficiently as targets pulsed with the ZnT8$_{186–194}$ peptide, while unpulsed K562-A2 control targets remained largely intact (Fig. 3A–B). In contrast, low avidity ZnT8$_{186–194}$-reactive clones were unable to lyse K562-A2/ZnT8 targets in the absence of exogenous ZnT8$_{186–194}$ peptide (Fig. 3C).

We then evaluated cytotoxicity against T1D-relevant targets by employing HLA-A2$^+$ ECN90 and control HLA-A2$^-$ EndoC-βH2 human β-cell lines. Although the ECN90 but not the EndoC-βH2 line expressed HLA Class I in the unstimulated state, expression levels were similarly upregulated by pretreatment with different cocktails of inflammatory cytokines, without inducing significant β-cell death (Fig. S4A–B). IFN-γ was chosen as the single cytokine that upregulated HLA Class I expression to comparable levels in both lines, and pretreatment was carried out for 18 h prior to a real-time cytotoxicity assay. As observed with K562-A2/ZnT8 targets, high avidity clones lysed unpulsed HLA-A2$^+$ ECN90 cells presenting naturally processed ZnT8-derived epitopes (Fig. 3D–E), while low avidity clones

displayed marginal lytic activity (Fig. 3F). Cytotoxicity increased in all cases with the addition of $ZnT8_{186–194}$ peptide, suggesting more limited natural presentation compared with ZnT8-transduced targets. Lysis of HLA-$A2^-$ EndoC-βH2 cells was negligible, and a control clone reactive to the melanocyte self-epitope $MelanA_{26–35}$ only lysed ECN90 cells in the presence of exogenous $MelanA_{26–35}$ peptide (Fig. 3G). Microscopic inspection confirmed the lysis measured in real-time cytotoxicity assays (Fig. S4C). β-cell lysis was not different between T1D and healthy clones, either in the absence or presence of exogenous $ZnT8_{186–194}$ peptide (Fig. 3H). Moreover, IFN-γ-pretreatment of HLA-$A2^+$ ECN90 cells neither upregulated ZnT8 protein expression (Fig. S4D) nor increased the functional activation of co-incubated $CD8^+$ T-cell clones (Fig. S4E–F). Collectively, these results demonstrate that $ZnT8_{186–194}$-reactive $CD8^+$ T cells display similar cytotoxicity in T1D and healthy subjects and that ZnT8 expression is not modulated by inflammation.

$ZnT8_{186–194}$-reactive $CD8^+$ T cells display private TCR gene usage but public CDR3β aminoacid sequences

Molecular analysis of expressed TCRα (*TRA*) and TCRβ (*TRB*) gene transcripts revealed that no sequences were shared (public) among $ZnT8_{186–194}$-reactive clones isolated from T1D or healthy subjects (Fig. S5). Of note, the 3 clones from patient D222D harbored an identical TCR. However, this observation did not affect our previous functional comparisons, because the measured parameters were even more similar between T1D and healthy donors when only one D222D clone was considered.

We then interrogated an *in-silico* database of *TRB* sequences compiled by high-throughput sequencing of naïve/terminal effector ($CD45RA^+CD45RO^-$) or central memory ($CD45RO^+CD45RA^-CD62L^{hi}$) $CD4^+$ and $CD8^+$ T cells obtained from HLA-$A2^+$ recent-onset T1D patients, at-risk aAb^+ and healthy subjects (Table S2). The D010R 1E2, H328C 8E8 and H034O 141B9 complementarity-determining region (CDR)3β aminoacid sequences were found among $CD8^+$ and $CD4^+$ T cells isolated from several individuals (Fig. 4A–C), mostly within the $CD45RA^+CD45RO^-$ pool for $CD8^+$ T cells. Several different *TRBV* genes were used in conjunction with these identical CDR3β loops to generate ‘mosaic’ sequences. The same CDR3β aminoacid sequences were detected *in-silico* among the polyclonal TCR repertoires compiled from conventional and regulatory $CD4^+$ and $CD8^+$ T cells isolated from pancreatic lymph node (PLN) and spleen samples by the Network for Pancreatic Organ Donors (nPOD) (Fig. 4D; n=67 identical CDR3β, n=6 identical TCRβ). Most of the $CD8^+$ T-cell hits in PLNs (11/15, 73%) were from HLA-$A2^+$ subjects, but with no obvious association with T1D.

To extend these findings, we developed D010R 1E2, H328C 8E8 and D222D *TRA* and *TRB* clonotype-specific TaqMan real-time quantitative PCR (qPCR) assays (Fig. S6A–B). Applied to $CD4^+$ and $CD8^+$ T-cell cDNA preparations from two independent cohorts of T1D (n=97 and n=53) and healthy subjects (n=97 and n=38), these assays detected the D010R and H328C *TRB* among $CD8^+$ T cells from a single HLA-$A2^+$ T1D patient in each case (Fig. S6C–D).

Collectively, these results show that $ZnT8_{186–194}$ recognition is mediated primarily by private clonotypes, some of which share CDR3β aminoacid sequences among individuals to form 'mosaic' TCRs.

Circulating islet-reactive CD8+ T cells display similar ex-vivo frequencies and a predominantly naïve phenotype in T1D and healthy subjects

In further experiments, we used *ex-vivo* combinatorial HLA-A2 MMr assays (9) to analyze $ZnT8_{186–194}$-reactive $CD8^+$ T cells in 39 HLA-$A2^+$ recent-onset T1D patients (16 children, 23 adults) and 39 age/sex-matched healthy donors (17 children, 22 adults) (Table S3, Fig. S7). Control specificities included $MelanA_{26–35}$, which is recognized by a large naïve pool in humans (13), and Flu $MP_{58–66}$, to which most individuals harbor Ag-experienced $CD8^+$ T cells reflecting prior viral exposure. Donors yielding $<3\times10^5$ total $CD8^+$ T cells or <5 MMr^+ cells were excluded from the analysis to avoid undersampling. Parallel ELISpot assays confirmed that $ZnT8_{186–194}$-reactive IFN-γ responses were more frequent in T1D *vs.* healthy donors (Fig. S8) (7). In contrast, similar frequencies of $ZnT8_{186–194}$ and $MelanA_{26–35}$ MMr^+CD8^+ T cells were detected in age-stratified T1D and healthy donors (Fig. 5A). Healthy chidren and adults displayed higher frequencies of Flu $MP_{58–66}$ MMr^+CD8^+ T cells compared with their age/sex-matched T1D counterparts, while children displayed ~4-fold higher frequencies of $ZnT8_{186–194}$ and $MelanA_{26–35}$ MMr^+CD8^+ T cells compared with adults, irrespective of T1D status.

Among $ZnT8_{186–194}$ MMr^+CD8^+ cells, the Ag-experienced fraction ($CD45RA^+CCR7^-$ or $CD45RA^-CCR7^{+/-}$) was similarly limited (generally ≤25% of all $ZnT8_{186–194}$ MMr^+ events) in T1D and healthy adults (Fig. 5B). In contrast, higher proportions of Ag-experienced $ZnT8_{186–194}$ MMr^+ cells were present in T1D children *vs.* adults, although these values were not different in healthy children. T1D children also harbored significantly higher proportions of Ag-experienced $ZnT8_{186–194}$ *vs.* $MelanA_{26–35}$ MMr^+ cells. $MelanA_{26–35}$-reactive $CD8^+$ T cells were mostly naïve, while Flu $MP_{58–66}$-reactive $CD8^+$ T cells were mostly Ag-experienced in all groups. Comparable results were obtained using the absolute frequencies of Ag-experienced MMr^+CD8^+ T cells (Fig. 5C).

Single-cell gene expression analysis of sorted $ZnT8_{186–194}$ MMr^+ cells (Fig. S9A) revealed few differences, with T1D patients displaying higher expression of the Th17-related aryl hydrocarbon receptor (*AHR*) and the mitotic aurora kinase A (*AURKA*) and lower expression of the transcriptional activator RAR related orphan receptor A (*RORA*). In line with our *in-vitro* data, clonotypic analyses of individual $ZnT8_{186–194}$ MMr^+CD8^+ T cells sorted *ex-vivo* yielded unique CDR3α and CDR3β sequences (Fig. S9B). Of the 21 CDR3β aminoacid sequences obtained, 7 (33%) were found in our *in-silico TRB* database across all subject groups (Fig. S9C). Among $CD8^+$ T cells, these 7 sequences were again most frequent within the $CD45RA^+CD45RO^-$ compartment, and predominantly found in T1D *vs.* healthy subjects. Preferential usage of certain *TRBV* (mostly *TRBV19*, 25%) and *TRAV* (mostly *TRAV12-2*, 38%) genes was observed (Fig. S9D–E), with *TRBV19* also shared among the $ZnT8_{186–194}$-reactive clones. However, only 8 out of 63 matching sequences (13%) expressed the *TRBV* gene of the corresponding $ZnT8_{186–194}$-reactive T cell. Thus,

despite biased *TRAV* and *TRBV* gene usage, the *ex-vivo* data confirmed that $ZnT8_{186–194}$ recognition is mediated primarily by private clonotypes expressing 'mosaic' TCRs.

Next, we used an extended combinatorial MMr panel to compare $ZnT8_{186–194}$-reactive $CD8^+$ T cells with those recognizing other immunodominant β-cell epitopes in adult donors (Fig. S10A). Assay reproducibility across panels was confirmed using separate blood draws from the same individuals (Fig. S10B). As observed for $ZnT8_{186–194}$, other β-cell-reactive $CD8^+$ T-cell populations displayed similar frequencies (typically 1–50 MMr^+ cells/10^6 $CD8^+$ T cells) in T1D and healthy adults (Fig. 5D). An exception was noted for $PPI_{15–24}$-reactive $CD8^+$ T cells, whose frequencies were lower than for other β-cell-reactive fractions, and higher in T1D *vs.* healthy donors. In all instances, the Ag-experienced fraction among MMr^+CD8^+ T cells was limited in both subject groups (Fig. 5E–F). The few children included in this extended analysis harbored β-cell-reactive $CD8^+$ T cells with a more Ag-experienced phenotype. $CD45RA^+CCR7^+$ islet-reactive cells were *bona fide* naïve, as they were largely $CD27^+CD28^+$ and $CD95^-$ (Fig. S11).

Collectively, these results show that circulating $CD8^+$ T cells reactive to $ZnT8_{186–194}$ and other β-cell epitopes occur at similar frequencies and exhibit a predominantly naïve phenotype in T1D and healthy adults, while higher frequencies of total and Ag-experienced $ZnT8_{186–194}$-reactive $CD8^+$ T cells are present in children, irrespective of T1D status.

Poor promiscuous ZnT8 gene expression in human thymic medullary epithelial cells (mTECs)

The combined observations that $CD8^+$ T cells reactive to $ZnT8_{186–194}$ and other β-cell epitopes are predominantly naïve and circulate at similar frequencies in T1D and healthy donors are compatible with frequent escape from thymic deletion due to poor islet Ag expression in mTECs (14). We tested this hypothesis by examining ZnT8 (*SLC30A8*) gene expression in total or immature (*AIRE*$^-$HLA Class II^{low}) *vs.* mature (*AIRE*$^+$HLA Class II^{high}) human mTECs from 5 children undergoing heart surgery. As mis-initiated mRNA transcription is described in mTECs (13, 15), forward primers were designed to identify potential alternative start sites *via* hybridization with exons 5, 6, 7 and 8 of the *SLC30A8* gene (Fig. 6A). The $ZnT8_{186–194}$ region is encoded by exons 7–8, with the exon 8 primer located just downstream. Combinations of these forward primers with reverse primers located either in exon 11 (Fig. 6B) or in the 3'-UTR (Fig. 6C) yielded the expected bands using human islet mRNA. However, mTECs did not express *SLC30A8*. One sample (#64) displayed a faint band amplified with the exon 8 forward primer, which matched *SLC30A8* by sequencing, suggesting low-level mis-initiated transcription starting at exon 8 (i.e. downstream of the $ZnT8_{186–194}$ region). Collectively, these results demonstrate that ZnT8 is poorly expressed in mTECs, and that *SLC30A8* transcription is limited to a mis-initiated mRNA isoform skipping the $ZnT8_{186–194}$ sequence.

Islet-reactive $CD8^+$ T cells circulate at similar frequencies irrespective of thymic expression of their cognate epitopes

In contrast to ZnT8, other β-cell Ags are expressed by mTECs, including PPI (16, 17), IA-2 (17, 18) and IGRP (19), or by thymic Ag-presenting cells, including GAD65 (20). Moreover,

circulating $PPI_{6–14}$-reactive $CD8^+$ T cells displayed higher frequencies than $PPI_{15–24}$-reactive $CD8^+$ T cells, despite the fact that the complete *INS* transcript incorporating both epitopes was detected in the thymus (Fig. 6D–E). In conjunction with the finding that circulating $CD8^+$ T cells reactive to $ZnT8_{186–194}$ and other islet epitopes also occur at similar frequencies (Fig. 5D), these observations suggest a limited role of thymic Ag gene expression in setting such frequencies.

Potential confounders in this scenario include the efficiency of epitope presentation and the odds of encountering cognate peptide-HLA complexes in the thymic environment. Accordingly, we compared the frequencies of islet-reactive $CD8^+$ T cells in age/sex-matched HLA-$A2^+$ and HLA-$A2^-$ healthy adults, reasoning that thymic deletion cannot occur in the absence of the appropriate HLA-A2 restriction (21). To exclude promiscuous presentation by non-HLA-A2 molecules, donors were selected based on HLA-A and HLA-B molecules incapable of binding the selected islet epitopes (Table S4). Moreover, all subjects were seronegative for Ebola (EboV) and hepatitis C virus (HCV). Representative flow cytometry plots are shown in Fig. S12. Except for $PPI_{6–14}$, HLA-A2-restricted islet-reactive $CD8^+$ T cells occurred at largely equivalent frequencies in HLA-$A2^+$ and HLA-$A2^-$ donors (Fig. 6F). Although higher overall relative to most islet specificities, the frequencies of MMr^+CD8^+ cells recognizing the HLA-A2-restricted foreign epitopes EboV $NP_{202–210}$ and HCV $PP_{1406–1415}$ were also similar between HLA-$A2^+$ and HLA-$A2^-$ groups. No significant phenotypic differences were observed between groups for any of these MMr^+CD8^+ T-cell populations (Fig. 6G). As expected, control Flu $MP_{58–66}$ MMr^+CD8^+ cells were more prevalent and more Ag-experienced in HLA-$A2^+$ donors.

Collectively, these findings suggest that thymic presentation of these islet epitopes does not trigger significant clonal deletion in HLA-$A2^+$ donors.

$ZnT8_{186–194}$-reactive $CD8^+$ T cells cross-recognize a Bacteroides stercoris mimotope

Although islet-reactive $CD8^+$ T cells were predominantly naïve in T1D and healthy adults, substantial Ag-experienced fractions were noted in some individuals, irrespective of disease status (Fig. 5B–5E). Moreover, $CD8^+$ T-cell frequencies correlated with the size of the Ag-experienced fraction for some individual ($ZnT8_{186–194}$, $IGRP_{265–273}$) and pooled islet epitopes (Fig. S13A–C), consistent with the patterns observed for Flu $MP_{58–66}$-reactive $CD8^+$ T cells (Fig. S13D). These observations raise the possibility of cross-priming by unrelated homologous epitopes (mimotopes). Indeed, sequence homology was observed between the $ZnT8_{186–194}$ epitope (VAANIVLTV) and a peptide (KAANIVLTV) derived from protein WP_060386636.1 of the intestinal commensal *Bacteroides stercoris*. To assess potential cross-reactivity, we performed *ex-vivo* MMr assays on duplicate PBMC samples. One sample was stained with pairs of $ZnT8_{186–194}$ MMrs, while the other was stained with one $ZnT8_{186–194}$ MMr and one *B. stercoris* MMr. Similar frequencies were detected for $ZnT8_{186–194}$-$ZnT8_{186–194}$ and $ZnT8_{186–194}$-*B. stercoris* double-MMr^+CD8^+ T cells in 3 of 4 donors (Fig. 7A). As a negative control, $ZnT8_{186–194}$-EboV $NP_{202–210}$ double-MMr^+CD8^+ T cells were undetectable (Fig. 7B), while EboV $NP_{202–210}$-EboV $NP_{202–210}$ double-MMr^+CD8^+ T cells were present at similar frequencies in duplicate samples (Fig. 7C). Cross-reactivity with the *B. stercoris* mimotope was confirmed for 1 of 4 $ZnT8_{186–194}$-reactive

CD8$^+$ T-cell clones *via* MMr co-staining (Fig. 7D) and *in-vitro* recall (Fig. 7E), with the *B. stercoris* mimotope displaying stronger agonist potency than the native ZnT8$_{186–194}$ peptide. Collectively, these results show that ZnT8$_{186–194}$-reactive CD8$^+$ T cells can cross-recognize a bacterial mimotope.

ZnT8$_{186–194}$-reactive cells are enriched in the pancreas of T1D donors

To reconcile the finding that equivalent frequencies of predominantly naïve islet-reactive CD8$^+$ T cells circulate in most individuals, we hypothesized that the T1D-relevant fraction may be sequestered in the pancreas. We therefore performed *in-situ* ZnT8$_{186–194}$ MMr staining on frozen pancreatic sections from HLA-A2$^+$ T1D (n=9), aAb$^+$ (n=9), non-diabetic (n=11) and type 2 diabetes (T2D) cases (n=3) from nPOD (Table S5). Representative images are shown in Fig. 8A–E, with scattered ZnT8$_{186–194}$ MMr$^+$ cells either within islets or the exocrine tissue. Consecutive sections from ZnT8$_{186–194}$ MMr$^+$ pancreata were probed with MelanA$_{26–35}$ MMrs, which, in conjunction with positive control vitiligo skin sections, confirmed staining specificity (Fig. 8F). Donor-matched PLN sections were stained in parallel (Fig. 8G–H). While ZnT8$_{186–194}$ MMr$^+$ cells were significantly more abundant than MelanA$_{26–35}$ MMr$^+$ cells in T1D, aAb$^+$ and non-diabetic cases, ZnT8$_{186–194}$ MMr$^+$ cells were enriched in the pancreata of T1D *vs.* non-diabetic and T2D cases (Fig. 8I). In contrast, ZnT8$_{186–194}$ MMr$^+$ cell were present at similar densities across all groups in PLN sections (Fig. 8J). Several of these nPOD cases were previously analyzed *in-silico* for the presence of ZnT8$_{186–194}$ CDR3β sequences in PLNs (Fig. 4D). These sequences were present in 4/5 cases with ZnT8 MMr$^+$ pancreata and 3/5 cases with ZnT8 MMr$^+$ PLNs (Table S5). A donor with chronic pancreatitis (#6288) and very high ZnT8$_{186–194}$-reactive CD3Rβ counts among spleen and PLN CD8$^+$ T cells also displayed high densities of ZnT8 MMr$^+$ cells in the pancreas. Collectively, these results show that ZnT8-reactive cells are preferentially enriched in the pancreas of T1D donors.

Discussion

In this study, we found that ZnT8$_{186–194}$-reactive CD8$^+$ T-cell clones exhibited heterogeneous functional profiles, but no consistent differences between T1D and healthy subjects. Most ZnT8$_{186–194}$-reactive clones originated from naïve precursors and expressed private TCRs. *Ex-vivo* analyses on larger donor cohorts revealed that the frequency of circulating ZnT8$_{186–194}$-reactive CD8$^+$ T cells was similar in age-matched T1D *vs.* healthy donors, but higher in children *vs.* adults, irrespective of T1D status. A similar pattern was noted for CD8$^+$ T cells recognizing the extra-pancreatic self-epitope MelanA$_{26–35}$, but the corresponding ZnT8$_{186–194}$-reactive populations were more Ag-experienced in T1D children. Thus, while most children harbor a larger autoimmune repertoire not restricted to islet Ags, the activation of the islet-reactive fraction occurs preferentially in T1D children, which may reflect a more aggressive islet autoimmunity leading to earlier disease onset. On the other hand, some Ag-experienced β-cell-reactive CD8$^+$ T cells were invariably detected in healthy donors, supporting the possibility that foreign epitopes may prime autoreactive clonotypes expressing promiscuous TCRs (22–24). Indeed, some ZnT8$_{186–194}$-reactive CD8$^+$ T-cell clonotypes were able to cross-recognize a *B. stercoris* mimotope. It is noteworthy that *B. stercoris* belongs to the *Bacteroidetes* phylum, which is enriched in the

gut microbiome of T1D (25) and at-risk aAb$^+$ subjects (26). Circulating CD8$^+$ T cells reactive to other HLA-A2-restricted β-cell epitopes were also detected at equivalent frequencies (1–50 MMr$^+$ cells/10^6 CD8$^+$ T cells) and with a predominantly naïve phenotype in T1D and healthy adults. This coherent pattern across islet specificities suggests that Ag-driven recruitment involves a limited fraction of naïve precursors, which fits with the paucity of public clonotypes found for ZnT8$_{186–194}$-reactive CD8$^+$ T cells, as reported for PPI$_{15–24}$ (4). Interestingly, the lower frequency of Flu-reactive CD8$^+$ T cells observed in T1D *vs.* healthy donors may reflect impaired anti-viral responses (27).

One strength of our *ex-vivo* studies is the highly specific and reproducible quantification of MMr$^+$ cells. The observed frequencies of β-cell-reactive CD8$^+$ T cells fall below previous estimates obtained without enrichment (4, 5), but mirror those described using stringent MMr-based magnetic enrichment (22). Although higher frequencies of β-cell-reactive CD8$^+$ T cells have been observed in T1D *vs.* healthy donors (5), our data align with another study reporting no difference (4). Importantly, this study validates comparisons based on dasatinib-enhanced MMr staining. Although the T1D children in our cohort had a longer disease duration than T1D adults, comparable age-related differences were observed in healthy donors, and similar trends remained when restricting the analysis to more recently diagnosed T1D children. Other studies reporting higher Ag-experienced β-cell-reactive CD8$^+$ T-cell fractions in T1D *vs.* healthy donors are potentially limited by undersampling and single MMr labeling (4). Moreover, such differences were not observed for all islet epitopes (4), and significant naïve fractions (~40%) were also present in T1D patients (4, 6).

T-cell precursors can escape thymic negative selection due to ‘blindspots’ that result from poor or incomplete expression of certain tissue Ags (13, 17, 28–30), due to alternative splicing and promoter usage and mis-initiated transcription (13–15, 30). These features favor the generation of truncated transcripts lacking certain T-cell epitopes, as observed for ZnT8. However, ZnT8$_{186–194}$-reactive CD8$^+$ T cells circulated at similar frequencies relative to other islet-reactive populations. Together with the finding that HLA-A2-restricted islet-reactive CD8$^+$ T cells circulated at similar frequencies in HLA-A2$^+$ and HLA-A2$^-$ donors, these results show that the thymus does not eliminate all autoreactive CD8$^+$ T cells. Nonetheless, thymic self-Ag expression may ‘prune’ autoreactive clonotypes bearing high-affinity TCRs (22, 31).

Perhaps the most outstanding question raised by our findings relates to the ‘benign’ state of islet autoimmunity ‘licensed’ by incomplete central tolerance. Evidence for such thymic defects in human T1D has been limited to *INS* polymorphisms, which rank second among T1D susceptibility loci after DQB1 and modulate thymic *INS* expression (16). Given the ongoing debate surrounding the role of thymic negative selection for autoreactive T cells (22, 32, 33), it is not altogether surprising that even this insulin paradigm does not fully explain T1D development. Indeed, homozygous *INS* susceptibility alleles are present in ~55% of Caucasians (34), yet very few develop T1D. We propose that incomplete clonal deletion of autoreactive T cells involves several other β-cell Ags besides insulin and is not restricted to T1D patients.

So what distinguishes benign from pathogenic autoimmune T cells? The evidence suggests that neither their blood frequency nor their phenotype are at play. However, naïve T cells circulate perpetually, in contrast to memory T cells. The body load of Ag-experienced autoreactive T cells may therefore be underestimated in the blood of diseased individuals due to tissue sequestration (35). In line with this, the number of $ZnT8_{186–194}$-reactive cells was higher than for Melan-$A_{26–35}$-reactive ones in the pancreas, similar between aAb^+ and non-diabetic donors, and enriched in the pancreas of T1D donors. Moreover, $ZnT8_{186–194}$-reactive $CD8^+$ T-cell clones displayed potent lytic activity, much higher than other islet specificities (1). While these findings suggest a pathogenic role for ZnT8-reactive $CD8^+$ T cells, their precise localization and Ag-experienced status within the pancreas and whether their numbers are inversely correlated with age as observed in the blood remain to be verified.

The second possibility is that autoimmune T cells may be differentially regulated in T1D and healthy donors (33, 36), either intrinsically (e.g. anergy or exhaustion) or extrinsically by regulatory T cells. In support of this notion, T1D-specific islet-reactive $CD8^+$ T cells have been repeatedly detected using functional IFN-γ ELISpot readouts (3, 7, 10), which employ unfractionated PBMCs, thus preserving regulatory networks. This observation also argues that peripheral blood can be informative under appropriate assay conditions. $ZnT8_{186–194}$-reactive $CD8^+$ T cells from T1D patients also expressed higher levels of aurora A kinase, which might hint at increased mitotic activity in the T1D setting. Mirroring this observation, an anergic phenotype has been reported for self-reactive $CD8^+$ T cells in non-autoimmune subjects (22, 36), which may be at least partially imprinted in the thymus (33, 37).

The third possibility is that the central diabetogenic ingredient may be enhanced β-cell vulnerability caused by islet inflammation in the face of similar autoimmune T-cell repertoires across individuals. In this scenario, tolerance to β-cell Ags may depend primarily on T-cell ignorance (32, 37). Three observations are noteworthy in this respect. First, the higher T1D risk at younger age contrasts with the lower risk of other autoimmune diseases, which may indicate greater β-cell vulnerability due to childhood stressors, such as islet-tropic enteroviruses and the metabolic demands imposed by growth. Second, high densities of $ZnT8_{186–194}$ MMr^+ cells were detected in the pancreas of an organ donor with chronic pancreatitis, suggesting that islet-reactive $CD8^+$ T cells can expand under inflammatory conditions that are not autoimmune *ab initio*. Third, $PPI_{15–24}$-reactive $CD8^+$ T cells were more frequent in T1D *vs.* healthy donors, with similar results reported for $PPI_{2–10}$ (22). These epitopes map to the PPI leader sequence, which may undergo enhanced processing and presentation under metabolic stress (1).

Collectively, the present data pose new challenges toward development of circulating T-cell biomarkers for T1D staging and suggest novel therapeutic strategies based on mimicking ‘benign’ autoimmunity or complementing incomplete central tolerance (38).

Supplementary Material

Refer to Web version on PubMed Central for supplementary material.

Acknowledgments

We thank C. Maillard, M. Scotto and S. Rozlan for technical assistance; Univercell Biosolutions for providing the ECN90 β-cell line; K. Kedzierska and her laboratory (University of Melbourne) for help with single-cell TCR sequencing; T. Brusko (University of Florida, Gainesville) for help with the nPOD TCR database; the CyBio platform of the Cochin Institute and DKFZ Flow Cytometry Core Facility for assistance with flow cytometry; T. Loukanov (University of Heidelberg) for providing human thymic tissue; K. Boniface and J. Seneschal (INSERM U1035, Bordeaux) for providing vitiligo skin sections; and S. You for reviewing the manuscript. Members of the ImMaDiab Study Group are listed in the Supplemental Acknowledgments.

Funding: This work was performed within the *Département Hospitalo-Universitaire* (DHU) AutHorS, supported by the *Programme Hospitalier de Recherche Clinique* ImMaDiab, Lilly France, the INSERM-Transfert Proof-of-Concept program acDC, the *Ile-de-France* CORDDIM, and by grants from the JDRF (1-PNF-2014-155-A-V, 2-SRA-2016-164-Q-R), the Aviesan/Astra Zeneca 'Diabetes and the Vessel Wall Injury' program, the *Société Francophone du Diabète*, the *Agence Nationale de la Recherche* (ANR-2015-CE17-0018-01), and the *Fondation pour la Recherche Médicale* (Equipe FRM DEQ20140329520), to RM; a JDRF Biomarkers grant (17-2012-598), to KC; an NIH R01 grant (DK052068), to HWD; Lilly and *Fondation Bettencourt-Schueller* funds, to RS; a European Research Council grant (ERC-2012-AdG), to BK; and funds from JDRF, the Wellcome Trust and the National Institute for Health Research (NIHR) Cambridge Biomedical Research Centre, to the JDRF/Wellcome Trust Diabetes and Inflammation Laboratory (CIMR, University of Cambridge), which provided PBMC samples from the JDRF D-GAP study. Samples from at-risk subjects were obtained through a TrialNet ancillary study to the TN-01 Pathway to Prevention study funded by NIH grants U01 DK061010, U01 DK061034, U01 DK061042, U01 DK061058, U01 DK085465, U01 DK085453, U01 DK085461, U01 DK085463, U01 DK085466, U01 DK085499, U01 DK085504, U01 DK085505, U01 DK085509, U01 DK103180, U01-DK103153, U01-DK085476, U01-DK103266 and by JDRF. DAP is a Wellcome Trust Senior Investigator (100326Z/12/Z). This research was performed with the support of the Network for Pancreatic Organ Donors with Diabetes (nPOD), a collaborative T1D research project funded by JDRF. Organ Procurement Organizations partnering with nPOD to provide research resources are listed at www.jdrfnpod.org/our-partners.php. This project has received funding from the Innovative Medicines Initiative 2 Joint Undertaking (INNODIA, no. 115797). This Joint Undertaking receives support from the Union's Horizon 2020 research and innovation programme and the European Federation of Pharmaceutical Industries and Associations, JDRF, and The Leona M. and Harry B. Helmsley Charitable Trust.

References and Notes

1. Skowera A, Ellis RJ, Varela-Calvino R, Arif S, Huang GC, Van-Krinks C, Zaremba A, Rackham C, Allen JS, Tree TI, Zhao M, Dayan CM, Sewell AK, Unger W, Drijfhout JW, Ossendorp F, Roep BO, Peakman M. CTLs are targeted to kill beta cells in patients with type 1 diabetes through recognition of a glucose-regulated preproinsulin epitope. J. Clin. Invest. 2008; 118:3390–3402. [PubMed: 18802479]
2. Coppieters KT, Dotta F, Amirian N, Campbell PD, Kay TW, Atkinson MA, Roep BO, von Herrath MG. Demonstration of islet-autoreactive CD8 T cells in insulitic lesions from recent onset and long-term type 1 diabetes patients. J. Exp. Med. 2012; 209:51–60. [PubMed: 22213807]
3. Mallone R, Martinuzzi E, Blancou P, Novelli G, Afonso G, Dolz M, Bruno G, Chaillous L, Chatenoud L, Bach JM, van Endert P. CD8+ T-cell responses identify beta-cell autoimmunity in human type 1 diabetes. Diabetes. 2007; 56:613–621. [PubMed: 17327428]
4. Skowera A, Ladell K, McLaren JE, Dolton G, Matthews KK, Gostick E, Kronenberg-Versteeg D, Eichmann M, Knight RR, Heck S, Powrie J, Bingley PJ, Dayan CM, Miles JJ, Sewell AK, Price DA, Peakman M. Beta-cell-specific CD8 T cell phenotype in type 1 diabetes reflects chronic autoantigen exposure. Diabetes. 2015; 64:916–925. [PubMed: 25249579]
5. Velthuis JH, Unger WW, Abreu JR, Duinkerken G, Franken K, Peakman M, Bakker AH, Reker-Hadrup S, Keymeulen B, Drijfhout JW, Schumacher TN, Roep BO. Simultaneous Detection of Circulating Autoreactive CD8+ T-Cells Specific for Different Islet Cell-Associated Epitopes Using Combinatorial MHC Multimers. Diabetes. 2010; 59:1721–1730. [PubMed: 20357361]
6. Luce S, Lemonnier F, Briand JP, Coste J, Lahlou N, Muller S, Larger E, Rocha B, Mallone R, Boitard C. Single insulin-specific CD8+ T cells show characteristic gene expression profiles in human type 1 diabetes. Diabetes. 2011; 60:3289–3299. [PubMed: 21998398]
7. Scotto M, Afonso G, Larger E, Raverdy C, Lemonnier FA, Carel JC, Dubois-Laforgue D, Baz B, Levy D, Gautier JF, Launay O, Bruno G, Boitard C, Sechi LA, Hutton JC, Davidson HW, Mallone

R. Zinc transporter (ZnT)8(186-194) is an immunodominant CD8+ T cell epitope in HLA-A2+ type 1 diabetic patients. Diabetologia. 2012; 55:2026–2031. [PubMed: 22526607]

8. Martinuzzi E, Afonso G, Gagnerault MC, Naselli G, Mittag D, Combadiere B, Boitard C, Chaput N, Zitvogel L, Harrison LC, Mallone R. acDCs enhance human antigen-specific T-cell responses. Blood. 2011; 118:2128–2137. [PubMed: 21715316]
9. Hadrup SR, Bakker AH, Shu CJ, Andersen RS, van VJ, Hombrink P, Castermans E, Thor SP, Blank C, Haanen JB, Heemskerk MH, Schumacher TN. Parallel detection of antigen-specific T-cell responses by multidimensional encoding of MHC multimers. Nat. Methods. 2009; 6:520–526. [PubMed: 19543285]
10. Enee E, Kratzer R, Arnoux JB, Barilleau E, Hamel Y, Marchi C, Beltrand J, Michaud B, Chatenoud L, Robert JJ, van Endert P. ZnT8 Is a Major CD8+ T Cell- Recognized Autoantigen in Pediatric Type 1 Diabetes. Diabetes. 2012; 61:1779–1784. [PubMed: 22586580]
11. Lissina A, Ladell K, Skowera A, Clement M, Edwards E, Seggewiss R, van den Berg HA, Gostick E, Gallagher K, Jones E, Melenhorst JJ, Godkin AJ, Peakman M, Price DA, Sewell AK, Wooldridge L. Protein kinase inhibitors substantially improve the physical detection of T-cells with peptide-MHC tetramers. J. Immunol. Methods. 2009; 340:11–24. [PubMed: 18929568]
12. Larsen M, Sauce D, Arnaud L, Fastenackels S, Appay V, Gorochov G. Evaluating cellular polyfunctionality with a novel polyfunctionality index. PLoS One. 2012; 7
13. Pinto S, Sommermeyer D, Michel C, Wilde S, Schendel D, Uckert W, Blankenstein T, Kyewski B. Misinitiation of intrathymic MART-1 transcription and biased TCR usage explain the high frequency of MART-1-specific T cells. Eur. J. Immunol. 2014; 44:2811–2821. [PubMed: 24846220]
14. Klein L, Kyewski B, Allen PM, Hogquist KA. Positive and negative selection of the T cell repertoire: what thymocytes see (and don't see). Nat. Rev. Immunol. 2014; 14:377–391. [PubMed: 24830344]
15. Villasenor J, Besse W, Benoist C, Mathis D. Ectopic expression of peripheral-tissue antigens in the thymic epithelium: probabilistic, monoallelic, misinitiated. Proc. Natl. Acad. Sci. U.S.A. 2008; 105:15854–15859. [PubMed: 18836079]
16. Pugliese A, Zeller M, Fernandez A Jr, Zalcberg LJ, Bartlett RJ, Ricordi C, Pietropaolo M, Eisenbarth GS, Bennett ST, Patel DD. The insulin gene is transcribed in the human thymus and transcription levels correlated with allelic variation at the INS VNTR-IDDM2 susceptibility locus for type 1 diabetes. Nat. Genet. 1997; 15:293–297. [PubMed: 9054945]
17. Gotter J, Brors B, Hergenhahn M, Kyewski B. Medullary epithelial cells of the human thymus express a highly diverse selection of tissue-specific genes colocalized in chromosomal clusters. J. Exp. Med. 2004; 199:155–166. [PubMed: 14734521]
18. Diez J, Park Y, Zeller M, Brown D, Garza D, Ricordi C, Hutton J, Eisenbarth GS, Pugliese A. Differential splicing of the IA-2 mRNA in pancreas and lymphoid organs as a permissive genetic mechanism for autoimmunity against the IA-2 type 1 diabetes autoantigen. Diabetes. 2001; 50:895–900. [PubMed: 11289059]
19. Dogra RS, Vaidyanathan P, Prabakar KR, Marshall KE, Hutton JC, Pugliese A. Alternative splicing of G6PC2, the gene coding for the islet-specific glucose-6- phosphatase catalytic subunit-related protein (IGRP), results in differential expression in human thymus and spleen compared with pancreas. Diabetologia. 2006; 49:953–957. [PubMed: 16520917]
20. Pugliese A, Brown D, Garza D, Murchison D, Zeller M, Redondo M, Diez J, Eisenbarth GS, Patel DD, Ricordi C. Self-antigen-presenting cells expressing diabetes-associated autoantigens exist in both thymus and peripheral lymphoid organs. J. Clin. Invest. 2001; 107:555–564. [PubMed: 11238556]
21. Rammensee HG, Bevan MJ. Evidence from in vitro studies that tolerance to self antigens is MHC-restricted. Nature. 1984; 308:741–744. [PubMed: 6232464]
22. Yu W, Jiang N, Ebert PJ, Kidd BA, Muller S, Lund PJ, Juang J, Adachi K, Tse T, Birnbaum ME, Newell EW, Wilson DM, Grotenbreg GM, Valitutti S, Quake SR, Davis MM. Clonal deletion prunes but does not eliminate self-specific alphabeta CD8(+) T lymphocytes. Immunity. 2015; 42:929–941. [PubMed: 25992863]

23. Tai N, Peng J, Liu F, Gulden E, Hu Y, Zhang X, Chen L, Wong FS, Wen L. Microbial antigen mimics activate diabetogenic CD8 T cells in NOD mice. J. Exp. Med. 2016; 213:2129–2146. [PubMed: 27621416]
24. Cole DK, Bulek AM, Dolton G, Schauenberg AJ, Szomolay B, Rittase W, Trimby A, Jothikumar P, Fuller A, Skowera A, Rossjohn J, Zhu C, Miles JJ, Peakman M, Wooldridge L, Rizkallah PJ, Sewell AK. Hotspot autoimmune T cell receptor binding underlies pathogen and insulin peptide cross-reactivity. J. Clin. Invest. 2016; 126:2191–2204. [PubMed: 27183389]
25. de Goffau MC, Fuentes S, van den Bogert B, Honkanen H, de Vos WM, Welling GW, Hyoty H, Harmsen HJ. Aberrant gut microbiota composition at the onset of type 1 diabetes in young children. Diabetologia. 2014; 57:1569–1577. [PubMed: 24930037]
26. de Goffau MC, Luopajarvi K, Knip M, Ilonen J, Ruohtula T, Harkonen T, Orivuori L, Hakala S, Welling GW, Harmsen HJ, Vaarala O. Fecal microbiota composition differs between children with beta-cell autoimmunity and those without. Diabetes. 2013; 62:1238–1244. [PubMed: 23274889]
27. Diepersloot RJ, Bouter KP, Beyer WE, Hoekstra JB, Masurel N. Humoral immune response and delayed type hypersensitivity to influenza vaccine in patients with diabetes mellitus. Diabetologia. 1987; 30:397–401. [PubMed: 3678660]
28. Giraud M, Taubert R, Vandiedonck C, Ke X, Levi-Strauss M, Pagani F, Baralle FE, Eymard B, Tranchant C, Gajdos P, Vincent A, Willcox N, Beeson D, Kyewski B, Garchon HJ. An IRF8-binding promoter variant and AIRE control CHRNA1 promiscuous expression in thymus. Nature. 2007; 448:934–937. [PubMed: 17687331]
29. Lv H, Havari E, Pinto S, Gottumukkala RV, Cornivelli L, Raddassi K, Matsui T, Rosenzweig A, Bronson RT, Smith R, Fletcher AL, Turley SJ, Wucherpfennig K, Kyewski B, Lipes MA. Impaired thymic tolerance to alpha-myosin directs autoimmunity to the heart in mice and humans. J. Clin. Invest. 2011; 121:1561–1573. [PubMed: 21436590]
30. Klein L, Klugmann M, Nave KA, Tuohy VK, Kyewski B. Shaping of the autoreactive T-cell repertoire by a splice variant of self protein expressed in thymic epithelial cells. Nat. Med. 2000; 6:56–61. [PubMed: 10613824]
31. Enouz S, Carrie L, Merkler D, Bevan MJ, Zehn D. Autoreactive T cells bypass negative selection and respond to self-antigen stimulation during infection. J. Exp. Med. 2012; 209:1769–1779. [PubMed: 22987800]
32. Legoux FP, Lim JB, Cauley AW, Dikiy S, Ertelt J, Mariani TJ, Sparwasser T, Way SS, Moon JJ. CD4+ T Cell Tolerance to Tissue-Restricted Self Antigens Is Mediated by Antigen-Specific Regulatory T Cells Rather Than Deletion. Immunity. 2015; 43:896–908. [PubMed: 26572061]
33. Davis MM. Not-So-Negative Selection. Immunity. 2015; 43:833–835. [PubMed: 26588773]
34. Bennett ST, Todd JA. Human type 1 diabetes and the insulin gene: principles of mapping polygenes. Annu. Rev. Genet. 1996; 30:343–370. [PubMed: 8982458]
35. Thome JJ, Yudanin N, Ohmura Y, Kubota M, Grinshpun B, Sathaliyawala T, Kato T, Lerner H, Shen Y, Farber DL. Spatial map of human T cell compartmentalization and maintenance over decades of life. Cell. 2014; 159:814–828. [PubMed: 25417158]
36. Maeda Y, Nishikawa H, Sugiyama D, Ha D, Hamaguchi M, Saito T, Nishioka M, Wing JB, Adeegbe D, Katayama I, Sakaguchi S. Detection of self-reactive CD8(+) T cells with an anergic phenotype in healthy individuals. Science. 2014; 346:1536–1540. [PubMed: 25525252]
37. Malhotra D, Linehan JL, Dileepan T, Lee YJ, Purtha WE, Lu JV, Nelson RW, Fife BT, Orr HT, Anderson MS, Hogquist KA, Jenkins MK. Tolerance is established in polyclonal CD4(+) T cells by distinct mechanisms, according to self-peptide expression patterns. Nat. Immunol. 2016; 17:187–195. [PubMed: 26726812]
38. Culina S, Gupta N, Boisgard R, Afonso G, Gagnerault MC, Dimitrov J, Osterbye T, Justesen S, Luce S, Attias M, Kyewski B, Buus S, Wong FS, Lacroix-Desmazes S, Mallone R. Materno-fetal transfer of preproinsulin through the neonatal Fc receptor protects from autoimmune diabetes. Diabetes. 2015; 64:3532–3542. [PubMed: 25918233]
39. Leisner C, Loeth N, Lamberth K, Justesen S, Sylvester-Hvid C, Schmidt EG, Claesson M, Buus S, Stryhn A. One-pot, mix-and-read peptide-MHC tetramers. PLoS One. 2008; 3:e1678. [PubMed: 18301755]

40. Ravassard P, Hazhouz Y, Pechberty S, Bricout-Neveu E, Armanet M, Czernichow P, Scharfmann R. A genetically engineered human pancreatic beta cell line exhibiting glucose-inducible insulin secretion. J. Clin. Invest. 2011; 121:3589–3597. [PubMed: 21865645]

41. Quigley MF, Almeida JR, Price DA, Douek DC. Unbiased molecular analysis of T cell receptor expression using template-switch anchored RT-PCR. Curr. Protoc. Immunol. 2011 Chapter 10, Unit 10.33.

42. Wang GC, Dash P, McCullers JA, Doherty PC, Thomas PG. T cell receptor alphabeta diversity inversely correlates with pathogen-specific antibody levels in human cytomegalovirus infection. Sci. Transl. Med. 2012; 4 128ra142.

43. Bonifacio E, Ziegler AG, Klingensmith G, Schober E, Bingley PJ, Rottenkolber M, Theil A, Eugster A, Puff R, Peplow C, Buettner F, Lange K, Hasford J, Achenbach P, Group P-PS. Effects of high-dose oral insulin on immune responses in children at high risk for type 1 diabetes: the Pre-POINT randomized clinical trial. JAMA. 2015; 313:1541–1549. [PubMed: 25898052]

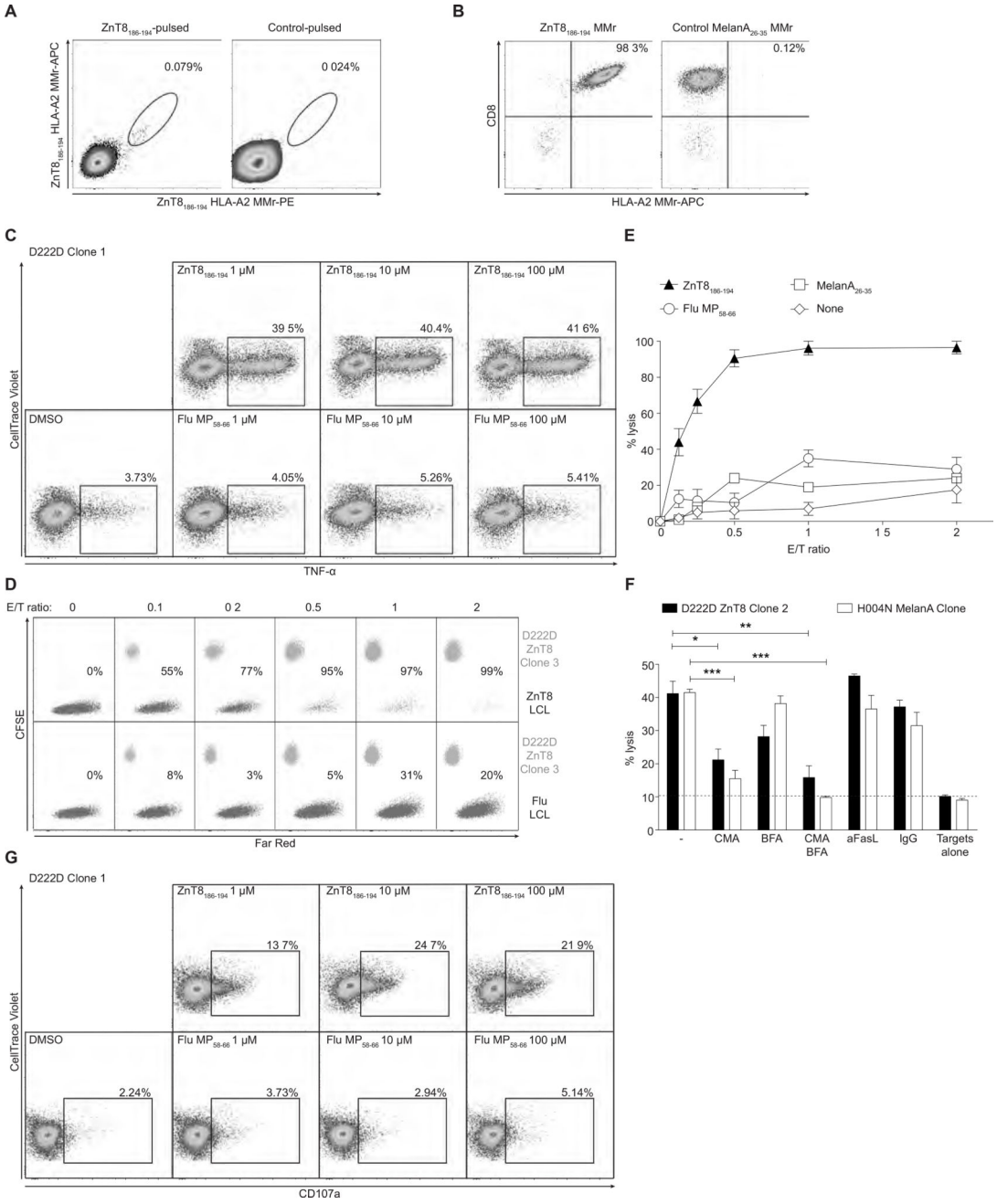

Fig. 1. ZnT8$_{186–194}$-reactive CD8$^+$ T-cell clones from patient D222D

(**A**) Frozen-thawed PBMCs were cultured with ZnT8$_{186–194}$ or no peptide and stained with PE/APC-labeled ZnT8$_{186–194}$ MMrs. (**B**) ZnT8$_{186–194}$ and control MMr stains for one clone obtained from single-sorted ZnT8$_{186–194}$/ZnT8$_{186–194}$ double-MMr$^+$ cells. (**C**) Percent intracellular TNF-α$^+$ D222D clone 1 cells stimulated for 6 h with K562-A2 cells pulsed with ZnT8$_{186–194}$ or Flu MP$_{58–66}$ peptide. (**D**) Percent lysis of FarRed-labeled LCL targets pulsed with ZnT8$_{186–194}$ (top) or Flu MP$_{58–66}$ peptide (bottom) and cultured for 24 h with CFSE-labeled D222D clone 3 at increasing E/T ratios. (**E**) Percent lysis of LCL targets cultured with D222D clones 1, 2 or 3 (mean±SEM; each clone is depicted in Fig. S1D–F).

(**F**) Lysis of cognate peptide-pulsed LCLs cultured for 4 h with D222D clone 2 or a MelanA$_{26–35}$-reactive clone (E/T 1/1) in the presence of concanamycin A (CMA), brefeldin A (BFA), CMA and BFA, anti-FasL or control IgG1. *p=0.015, **p=0.009, ***p<0.001 by Student's t test. Results are mean±SEM of triplicate measurements from one of three experiments. (**G**) Percent surface CD107a$^+$ D222D clone 1 cells stimulated as in (C). For panels A, C, G, gate is on viable CD8$^+$ cells.

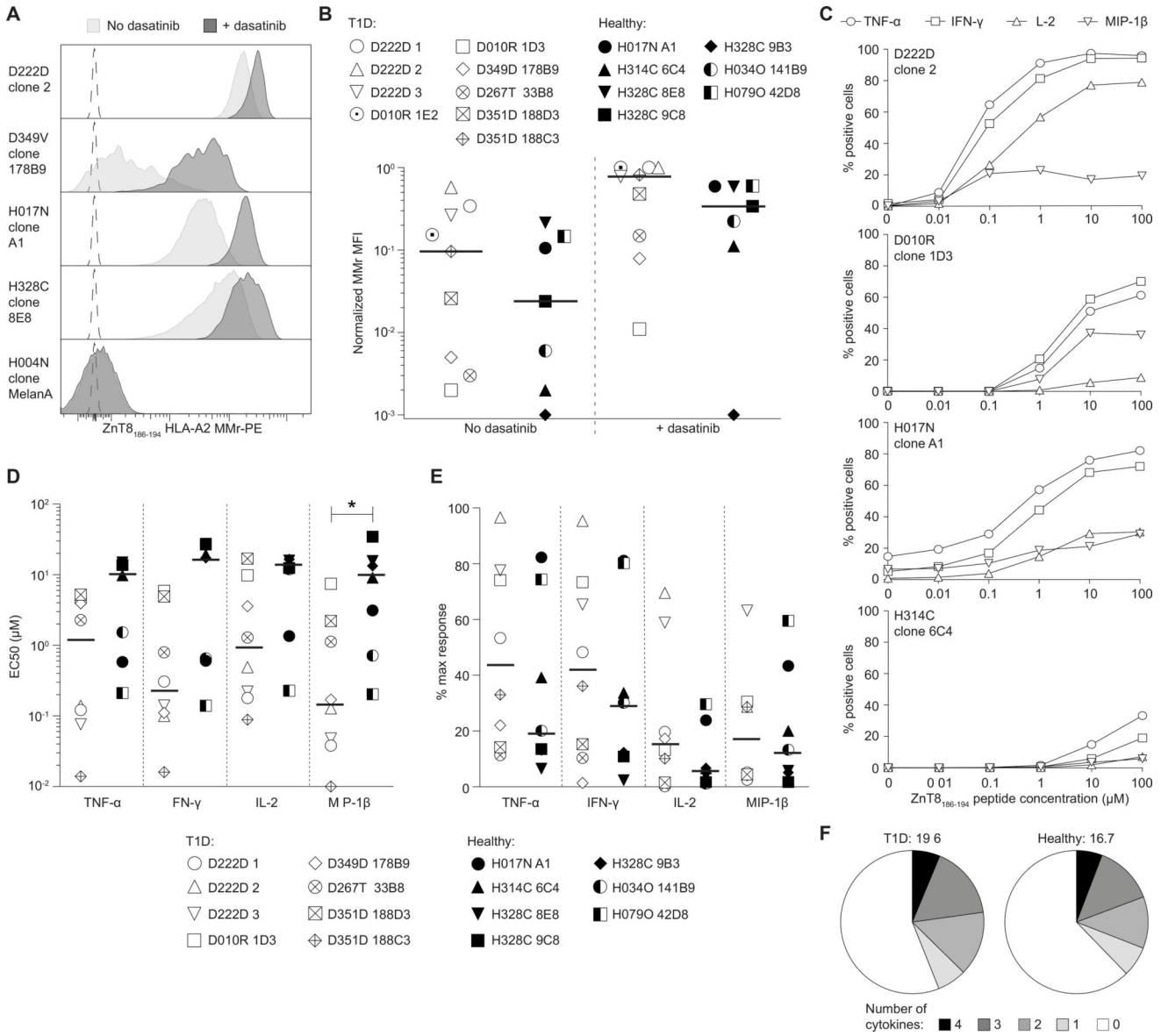

Fig. 2. Ag avidity, Ag sensitivity and polyfunctionality of ZnT8$_{186–194}$-reactive CD8$^+$ T-cell clones

(**A**) ZnT8$_{186–194}$ MMr staining in the absence (light grey) or presence (dark grey) of dasatinib. The dotted profile indicates the unstained control. (**B**) ZnT8$_{186–194}$ MMr median fluorescence intensity (MFI) for the indicated clones in the absence (left) or presence (right) of dasatinib. Bars indicate median values. Results are representative of two separate experiments. (**C**) The indicated clones were stimulated for 6 h with ZnT8$_{186–194}$-pulsed K562-A2 cells and percent cytokine$^+$ cells out of viable CD8$^+$ cells calculated. Results are representative of three independent experiments. (**D–E**) Half maximal effective peptide concentration (EC50; D) and maximal cytokine response (percent cytokine$^+$ cells at optimal peptide concentrations; E) for clones stimulated as above. Bars indicate median values. Results are representative of two to four separate experiments. *p=0.014 by Mann-Whitney test. (**F**) Polyfunctionality distribution of T1D (left) and healthy clones (right). Percent T

cells producing 0 to 4 cytokines among TNF-α, IFN-γ, IL-2 and MIP-1β upon exposure to $ZnT8_{186–194}$-pulsed K562-A2 cells (100 μM) are shown.

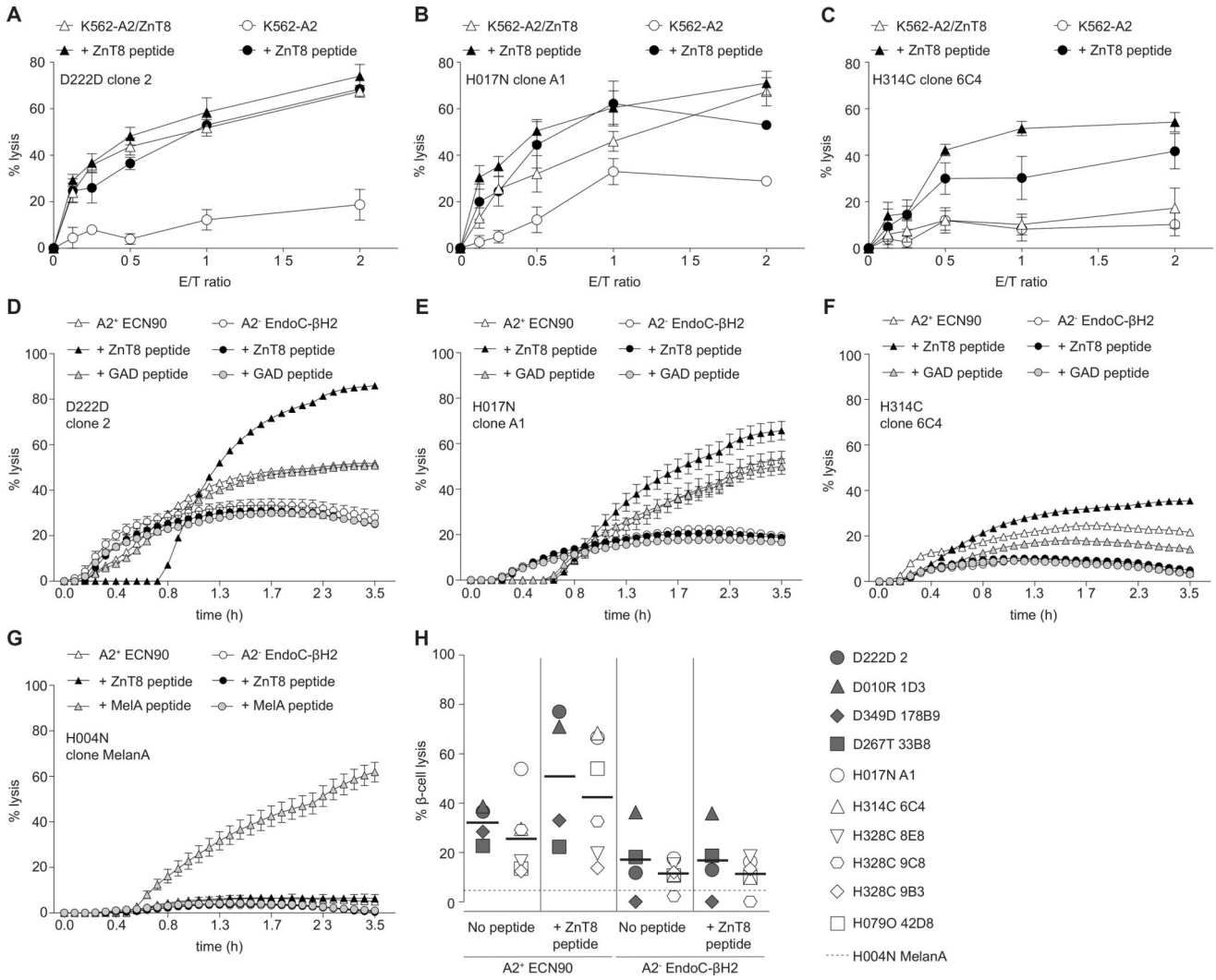

Fig. 3. Target cell lysis by ZnT8$_{186–194}$-reactive CD8$^+$ T-cell clones

(**A–C**) Lysis of K562-A2 cells transfected (open triangles) or not (open circles) with a full-length ZnT8 plasmid and cultured for 24 h with clones D222D 2 (A), H017N A1 (B) or H314C 6C4 (C). Filled symbols indicate ZnT8$_{186–194}$-pulsed target cells (10 μM). Results are presented as mean±SEM of triplicate wells from two separate experiments. (**D–G**) Real-time cytotoxicity for the indicated clones *vs.* HLA-A2$^+$ ECN90 (white triangles) or control HLA-A2$^-$ EndoC-βH2 β-cell targets (white circles) (E/T 2/1). Black and grey symbols indicate the corresponding targets pulsed with 10 μM ZnT8$_{186–194}$ or GAD$_{114–122}$ peptide, respectively. Mean±SEM of triplicate measurements are shown at each time point. Results are representative of at least two separate experiments. (**H**) Percent maximal HLA-A2$^+$ ECN90 and HLA-A2$^-$ EndoC-βH2 β-cell lysis by the indicated clones (T1D, grey symbols; healthy, white symbols; control, horizontal dotted line) in the absence or presence of ZnT8$_{186–194}$ peptide. Bars indicate median values. Lysis was calculated from the cytotoxicity profiles as in panels D–G.

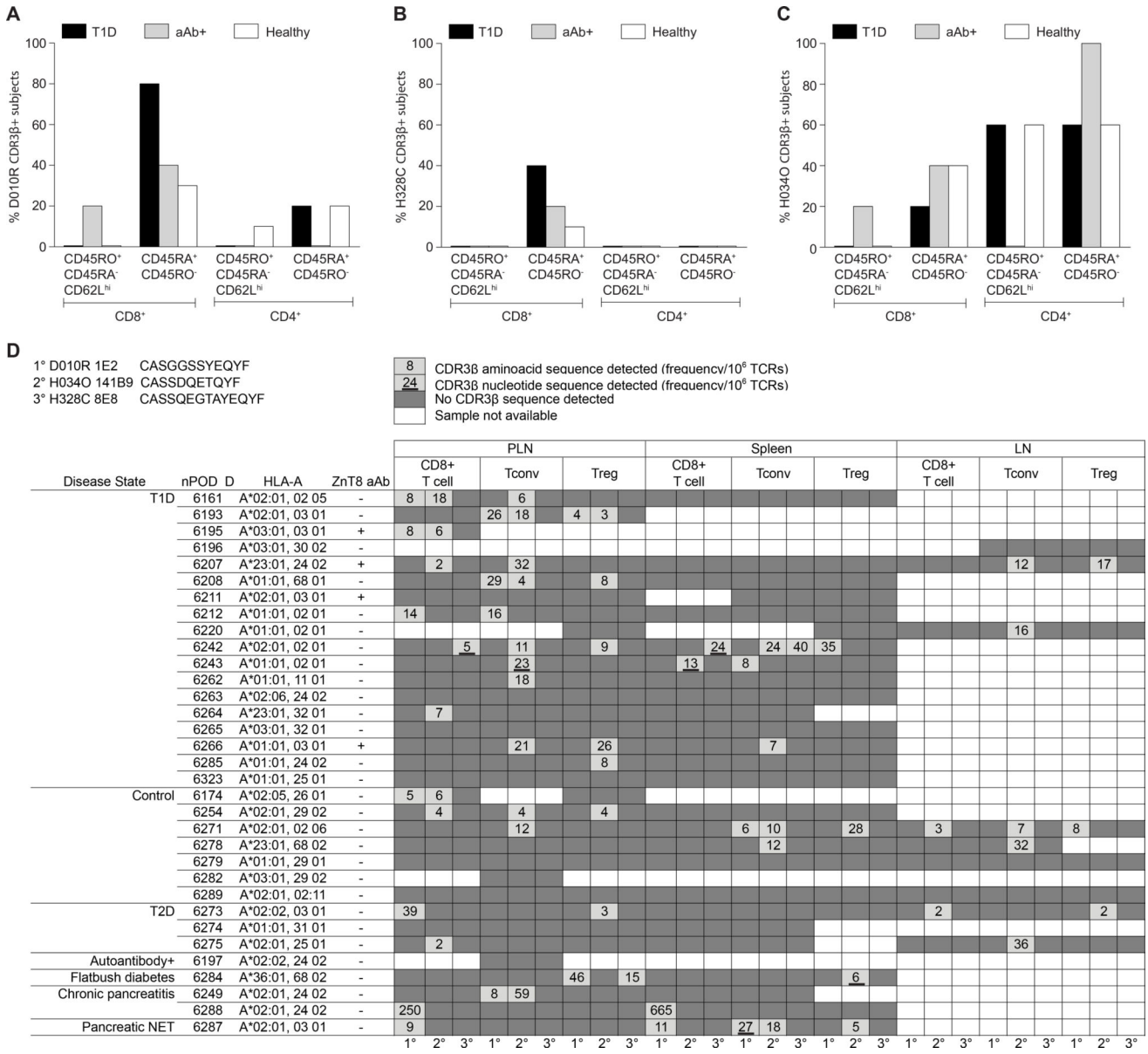

Fig. 4. *In-silico* search for CDR3β aminoacid sequences from ZnT8$_{186–194}$-reactive CD8$^+$ T-cell clones

(**A–C**) Prevalence of the CDR3β aminoacid sequences from clones D010R 1E2 (A), H328C 8E8 (B) and H034O 141B9 (C) among HLA-A2$^+$ T1D (n=5), aAb$^+$ (n=5) and healthy subjects (n=10), as assessed by *in-silico* analysis of TCRβ repertoires obtained from the indicated CD8$^+$ and CD4$^+$ T-cell subsets. (**D**) *In-silico* search for the same CDR3β aminoacid sequences in the repertoire of CD8$^+$, conventional CD4$^+$ (Tconv; CD127$^+$) and regulatory CD4$^+$ (Treg; CD25$^+$CD127$^-$) T cells obtained from nPOD PLN, spleen and inguinal lymph node (ILN) samples *via* the online database http://clonesearch.jdrfnpod.org. For each cell type and tissue, the first, second and third columns refer to clones D010R 1E2, H034O 141B9 and H328C 8E8, respectively. Dark and light grey cells indicate negative and positive samples, respectively. Frequencies per 10^6 TCRs are annotated, and underlining

indicates samples with a nucleotide sequence match. White cells indicate unavailable samples. Pancreatic NET, neuro-endocrine tumor.

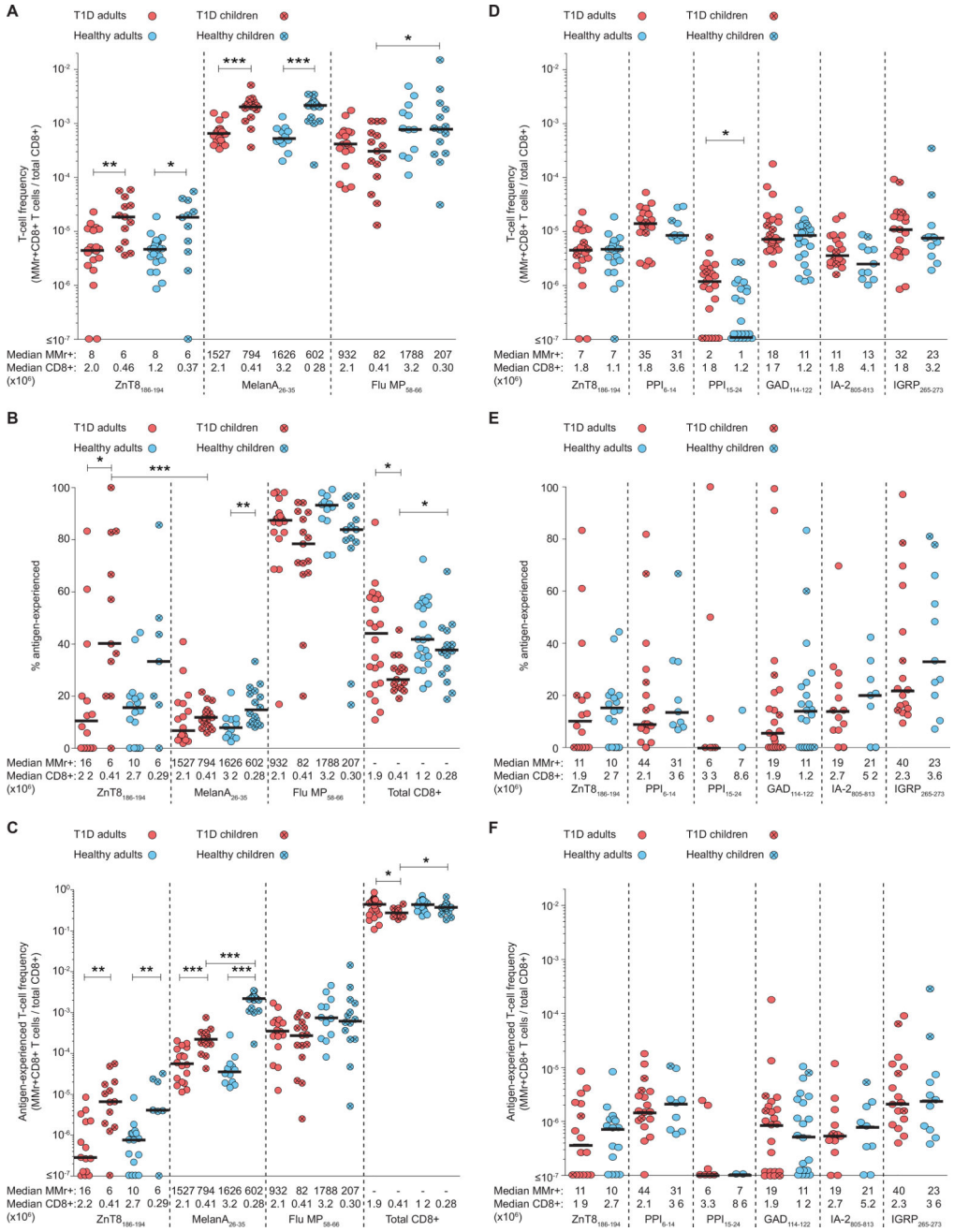

Fig. 5. *Ex-vivo* frequencies and Ag-experienced phenotypes of circulating islet-reactive CD8$^+$ T cells

(**A**) ZnT8$_{186–194}$, MelanA$_{26–35}$ and Flu MP$_{58–66}$ MMr$^+$CD8$^+$ cells were stained *ex-vivo* and counted (see Fig. S7). Frequencies out of total CD8$^+$ T cells are depicted for T1D adults (red circles), T1D children (crossed red circles), age/sex-matched healthy adults (blue circles) and children (crossed blue circles). *p≤0.05, **p=0.002, ***p≤0.0003. (**B**) Percent Ag-experienced cells out of total MMr$^+$ cells. *p≤0.03, **p=0.004, ***p=0.0007. (**C**) Absolute frequencies of the corresponding Ag-experienced fractions. *p≤0.03, **p≤0.01, ***p≤0.0001. (**D**) MMr$^+$CD8$^+$ cells reactive to the indicated islet epitopes were stained *ex-*

vivo and counted (see Fig. S10A). Frequencies out of total $CD8^+$ T cells are depicted as in panel A. *p=0.02. (**E**) Percent Ag-experienced cells out of total MMr^+ cells. (**F**) Absolute frequencies of the corresponding Ag-experienced fractions. Bars display median values. The median number of MMr^+ events and total $CD8^+$ T cells analyzed are indicated for each distribution. Significance was determined using the Mann-Whitney test. For panels A and D, data-points with <300,000 $CD8^+$ T cells and <5 MMr^+ cells were excluded. For panels B–C and E–F, data-points with <5 MMr^+ cells were excluded.

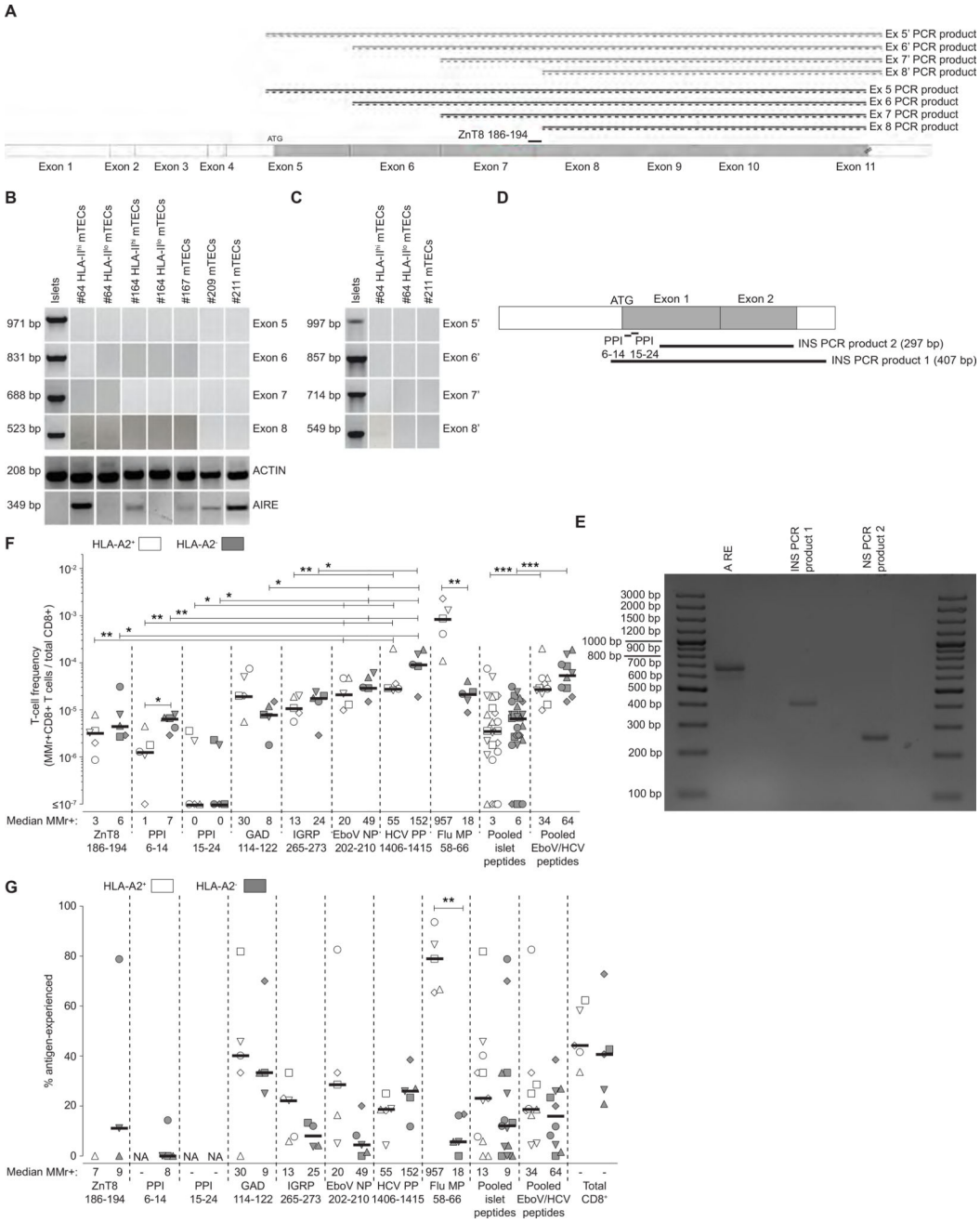

Fig. 6. *SLC30A8* and *INS* gene expression in mTECs and circulating islet-reactive CD8$^+$ T-cell frequencies in HLA-A2$^+$ and HLA-A2$^-$ healthy donors

(**A**) *SLC30A8* RT-PCR strategy. Forward primers spanned exons 5 to 8, reverse primers spanned either exon 11 or the 3'-UTR. The position of the ZnT8$_{186–194}$-coding region is shown. (**B**) *SLC30A8* expression in mTECs, using the indicated forward primers and the exon 11 reverse primer. (**C**) *SLC30A8* expression in mTECs from donor #64 (previously testing positive with the exon 8 forward primer) and #211 (previously testing negative), using the 3'-UTR reverse primer. (**D**) *INS* RT-PCR strategy. Forward primers spanned both or neither of the PPI$_{6–14}$ and PPI$_{15–24}$ regions, reverse primers spanned either the 3'-UTR or

exon 2 (PCR products 1 and 2, respectively). (**E**) *INS* expression in thymuses pooled from 5–8 donors. (**F**) *Ex-vivo* MMr^+CD8^+ cell frequencies in age/sex-matched, EboV- and HCV-seronegative HLA-$A2^+$ and HLA-$A2^-$ healthy donors. (**G**) Percent Ag-experienced MMr^+ cells. Bars indicate median values. The median number of MMr^+ events is indicated, with a median of 1×10^6 total $CD8^+$ T cells analyzed. *$p\leq0.03$, **$p=0.008$, ***$p\leq0.0004$ by Mann-Whitney test. For panels G, data points with <5 MMr^+ cells were excluded. NA, not available.

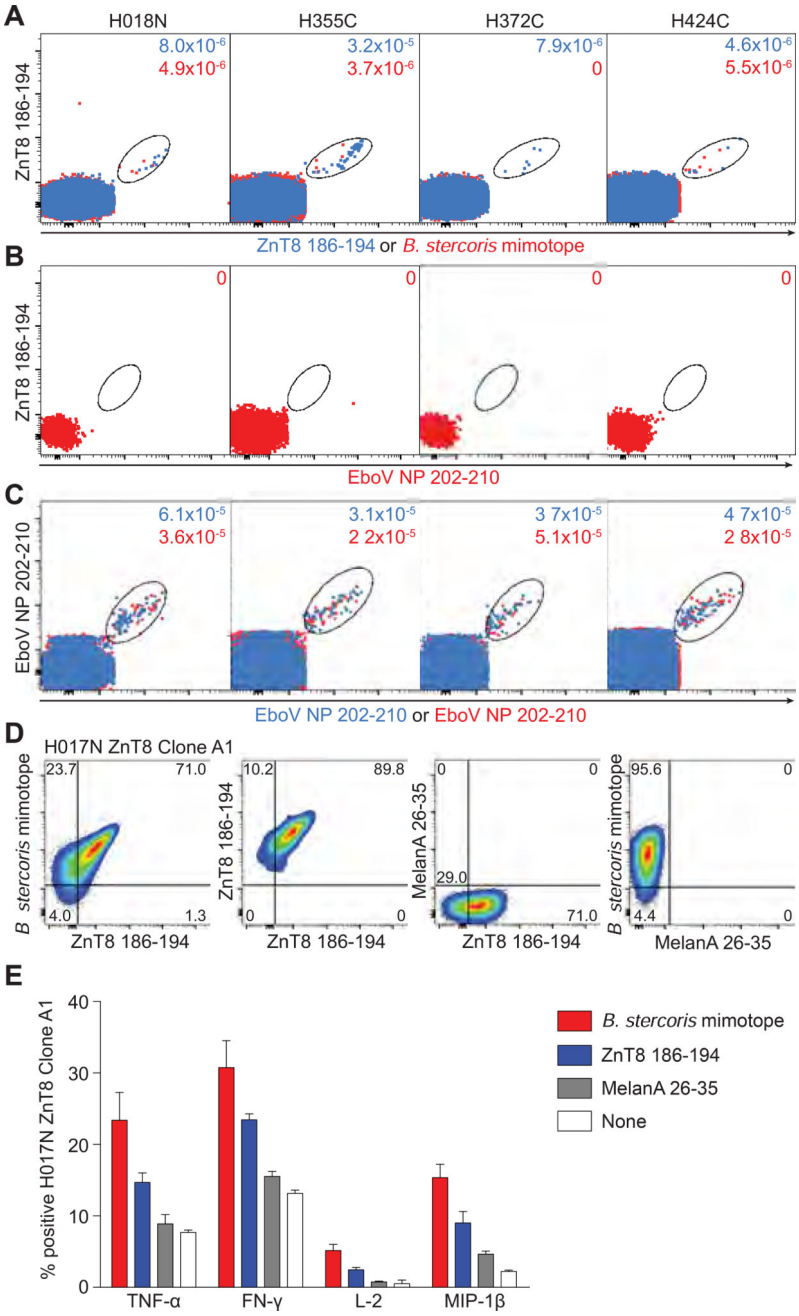

Fig. 7. $ZnT8_{186–194}$-reactive $CD8^+$ T cells cross-recognize a *B. stercoris* mimotope

(**A–C**) Four donors with sizable $ZnT8_{186–194}$ MMr^+CD8^+ T-cell fractions were selected. A first PBMC aliquot received PE/BV786-labeled $ZnT8_{186–194}$ MMrs and PE/BV711-labeled EboV $NP_{202–210}$ MMrs. For the second aliquot, PE-labeled *B. stercoris* MMrs replaced the PE-labeled $ZnT8_{186–194}$ MMrs. (**A**) Overlay of $ZnT8_{186–194}$/$ZnT8_{186–194}$ MMr^+ (blue) and $ZnT8_{186–194}$/*B. stercoris* MMr^+ cells (red). (**B**) Negative control staining of $ZnT8_{186–194}$/EboV $NP_{202–210}$ MMr^+ cells. (**C**) Positive control staining of EboV $NP_{202–210}$/EboV $NP_{202–210}$ MMr^+ cells from the first and second aliquot. The frequencies of MMr^+ out of total $CD8^+$ T cells are indicated. (**D**) Four $ZnT8_{186–194}$-reactive $CD8^+$ T-cell clones (D222D

2, D349D 178B9, H017N A1, H328C 9C8) were stained with BV786/PE-labeled $ZnT8_{186–194}$, PE-labeled *B. stercoris* and BV650-labeled $MelanA_{26–35}$ MMrs. The $ZnT8_{186–194}$/*B. stercoris* cross-reactive clone H017N is shown, from left to right: $ZnT8_{186–194}$/*B. stercoris* MMr^+; $ZnT8_{186–194}$/$ZnT8_{186–194}$ MMr^+; and negative control $ZnT8_{186–194}$/$MelanA_{26–35}$ and *B. stercoris*/$MelanA_{26–35}$ MMr^+ cells. (**E**) The H017N clone was stimulated with peptide-pulsed LCLs (0.1 μM, 6 h). Percent $cytokine^+$ cells are shown as mean±SEM of two experiments. p=0.008 for Wilcoxon signed-rank comparison of pooled cytokine responses between *B. stercoris* and $ZnT8_{186–194}$, $MelanA_{26–35}$ or no peptide, and between $ZnT8_{186–194}$ and $MelanA_{26–35}$ or no peptide.

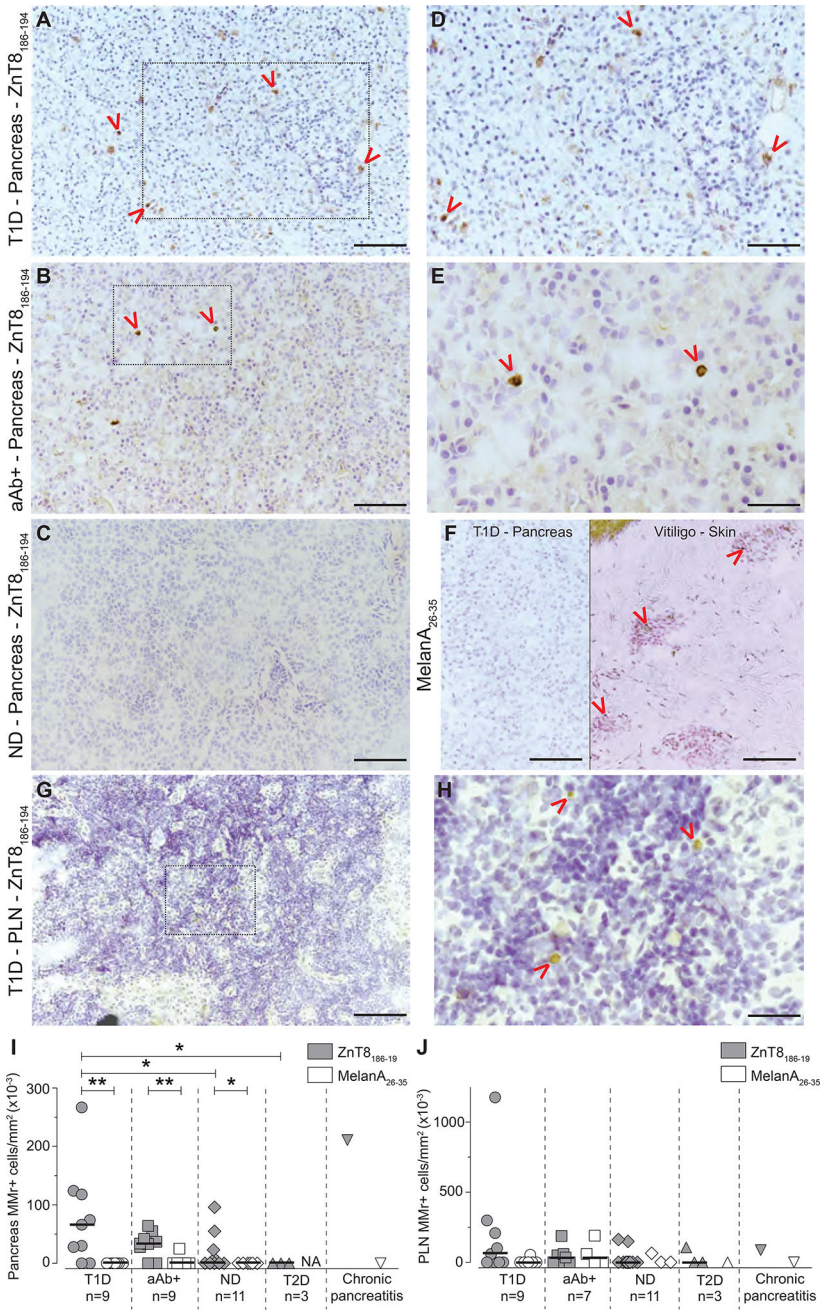

Fig. 8. *In-situ* ZnT8$_{186–194}$ MMr staining of nPOD pancreas and PLN sections

(**A–E**) Representative pancreas images (20X magnification; scale bar 100 μm) from cases T1D #6161 (A), aAb$^+$ #6347 (B) and non-diabetic (ND) #6289 (C). Red arrows indicate MMr$^+$ cells and the dotted areas of panels A–B are magnified in panels D (scale bar 80 μm) and E (scale bar 50 μm), respectively. (**F**) Consecutive sections from ZnT8$_{186–194}$ MMr$^+$ pancreata were probed with negative control MelanA$_{26–35}$ MMrs. A representative image from T1D case #6211 is shown on the left, and a positive control staining on skin sections from a vitiligo patient is shown on the right (20X; scale bar 100 μm). (**G**) Representative PLN image (20X; scale bar 100 μm) from T1D case #6161. (**H**) Magnification of the dotted

area of panel G (scale bar 40 μm). (**I–J**) Number of $ZnT8_{186–194}$ and $MelanA_{26–35}$ MMr^{+} cells/mm^2 section area of pancreas (I) and PLNs (J). Each point represents an individual case (detailed in Table S5). Bars indicate median values. *$p \leq 0.05$, **$p \leq 0.009$ by Mann-Whitney test. NA, not assessed.